Integrated IMU and Radiolocation-based Navigation Using A Rao-Blackwellized Particle Filter

William Wei-Liang Li*, *Member, IEEE,* Ronald A. Iltis*, *Senior Member, IEEE,* and Moe Z. Win†, *Fellow, IEEE*

*Department of Electrical and Computer Engineering, University of California, Santa Barbara, CA 93106 USA
†Laboratory for Information and Decision Systems, Massachusetts Institute of Technology, Cambridge, MA 02139 USA

Abstract—In this paper, we develop a cooperative IMU/radio-location-based navigation system, where each node tracks the location not only based on its own measurements, but also via collaboration with neighbor nodes. The key problem is to design a nonlinear filter to fuse IMU and radiolocation information. We apply the Rao-Blackwellization method by using a particle filter and parallel Kalman filters for the estimation of orientation and other states (i.e., position, velocity, etc.), respectively. The proposed method significantly outperforms the extended Kalman filter (EKF) in the set of simulations here.

Index Terms—Cooperative localization, navigation, inertial measurement unit (IMU), information fusion, particle filter.

I. INTRODUCTION

Navigation enables numerous emerging wireless applications in commercial, public and military operations [1]–[4]. Conventional techniques based on the global positioning system (GPS) often fail to provide reliable position information in harsh and indoor environments, due to the inability of GPS signals to penetrate many obstacles. For these reasons, GPS-less navigation using compact IMUs [5]–[8] and ultrawideband-based radiolocation [9]–[11] is of great current interest.

Inertial measurement units (IMU) have been widely adopted in assisting navigation when the GPS signal is severely attenuated and distorted. The IMU usually contains accelerometer and gyroscope sensors, measuring force and angular velocity, respectively. However, IMU-based navigation is accurate only for a short period of time due to the cubic error drift [12]. Recent work [12], [13] considered a foot-mounted IMU strategy which adopts step detection to correct the error. The drawback is that the step detection could introduce additional bias and drift, which degrades the navigation performance.

The accuracy of IMU-based navigation depends on the IMU model and filter design. In [14], a linear Gaussian drift model for IMU-derived position estimates is assumed by a Kalman filter. However, a more realistic IMU model is nonlinear due to coupling of orientation and acceleration measurements. The extended Kalman filter (EKF) is commonly used in such navigation applications due to its relative simplicity [5], [13], [15], [16]. It is well known that the EKF is suboptimal

for such nonlinear applications and can generate divergent position/orientation estimates. Hence, the design of a more accurate, but computationally tractable nonlinear IMU filter remains a significant challenge.

In this paper, we develop a cooperative IMU-based navigation system, which fuses IMU measurement and radiolocation infomation to track the mobile node positions. The major contributions are summarized as follows:

- We design a Rao-Blackwellized particle filter (RB-PF) for IMU-based navigation. The proposed method significantly outperforms the EKF in the simulations here, and achieves much better convergence.
- We integrate the position information derived from IMU and radiolocation to achieve highly accurate navigation in both line-of-sight (LOS) and non-line-of-sight (NLOS) environments.
- We improve the navigation accuracy by using cooperative localization among the mobile nodes. The simulation results validate the importance of cooperation in navigation.

II. DYNAMIC AND MEASUREMENT MODEL FOR IMU

In this section, we describe the process model and the measurement model of the IMU. We define $\varphi_k(n)$ as the IMU orientation with respect to the reference frame, and $\boldsymbol{x}_k(n)$ as a state vector containing position, velocity, acceleration, and the first-order derivative of orientation, given by[1]

$$\boldsymbol{x}_k(n) = [\, x_k(n), y_k(n), \dot{x}_k(n), \dot{y}_k(n), \ddot{x}_k(n), \ddot{y}_k(n), \dot{\varphi}_k(n) \,]^{\mathrm{T}}.$$

The IMU process model can be written as

$$\boldsymbol{x}_k(n+1) = \mathbf{F}\boldsymbol{x}_k(n) + \mathbf{G}\mathbf{w}_k(n) \tag{1}$$

$$\varphi_k(n+1) = \varphi_k(n) + T\dot{\varphi}_k(n) + \frac{T^2}{2}\mathbf{w}_{k,\varphi}(n) \tag{2}$$

where

$$\mathbf{F} = \begin{bmatrix} \mathbf{I}_2 & T\mathbf{I}_2 & T^2/2\mathbf{I}_2 & 0 \\ \mathbf{0}_2 & \mathbf{I}_2 & T\mathbf{I}_2 & \vdots \\ \mathbf{0}_2 & \mathbf{0}_2 & \mathbf{I}_2 & 0 \\ 0 & \dots & 0 & 1 \end{bmatrix}, \quad \mathbf{G} = \begin{bmatrix} T^3/6\mathbf{I}_2 & 0 \\ T^2/2\mathbf{I}_2 & \vdots \\ T\mathbf{I}_2 & 0 \\ 0 & 0 & T \end{bmatrix}$$

with the sample time T, and $\mathbf{I}_n$ and $\mathbf{0}_n$ denoting the $n \times n$ unit matrix and zero matrix, respectively. The noise vector

[1]We focus on the 2-D case, and the model can be extended to the 3-D case.

$\mathbf{w}_k(n) = [\mathrm{w}_{k,x}(n), \mathrm{w}_{k,y}(n), \mathrm{w}_{k,\varphi}(n)]^\mathrm{T}$ is an i.i.d. Gaussian sequence, where $[\mathrm{w}_{k,x}(n), \mathrm{w}_{k,y}(n)]^\mathrm{T} \sim \mathcal{N}(\mathbf{0}, \sigma_k^2 \mathbf{I}_2)$ and $\mathrm{w}_{k,\varphi}(n) \sim \mathcal{N}(0, \sigma_{k,\varphi}^2)$ with standard deviation in m/s³ and rad/s², respectively. The covariance matrix of $\mathbf{w}_k(n)$ is denoted as $\boldsymbol{Q}_k$.

The IMU measurements include the angular velocity ω_k and the normalized force $\boldsymbol{f}_k$, both with respect to the body frame given by[2]

$$\boldsymbol{z}_k(n) = \begin{bmatrix} \omega_k(n) \\ \boldsymbol{f}_k(n) \end{bmatrix} = \mathbf{H}(\varphi_k(n))\boldsymbol{x}_k(n) + \mathbf{v}_k(n) \quad (3)$$

where

$$\mathbf{H}(\varphi_k(n)) = \begin{bmatrix} 0 & \cdots & 0 & 0 & 1 \\ \mathbf{0}_2 & \mathbf{0}_2 & \cos\varphi_k(n) & -\sin\varphi_k(n) & 0 \\ & & \sin\varphi_k(n) & \cos\varphi_k(n) & 0 \end{bmatrix}$$

and the additive IMU noise $\mathbf{v}_k(n) = [\mathrm{v}_{k,\omega}(n), \mathbf{v}_{k,f}(n)]^\mathrm{T}$ is an i.i.d. Gaussian sequence with $\mathrm{v}_{k,\omega}(n) \sim \mathcal{N}(0, \sigma_{k,\omega}^2)$ and $\mathbf{v}_{k,f}(n) \sim \mathcal{N}(\mathbf{0}, \sigma_{k,f}^2 \mathbf{I}_2)$. The covariance matrix of $\mathbf{v}_k(n)$ is denoted as $\boldsymbol{R}_k$.

Remark 1: The IMU measurement model in (3) is a nonlinear function of both the orientation $\varphi_k(n)$ and state vector $\boldsymbol{x}_k(n)$.

III. RAO-BLACKWELLIZED PARTICLE FILTER FOR IMU-BASED NAVIGATION

Due to the nonlinearity in the orientation in (3), we decompose the navigation problem using a separate nonlinear model of $\varphi_k(n)$, and adopt particle filters for orientation estimation. Once the particle streams are specified, the remaining estimation problems become linear Gaussian solvable by parallel Kalman filters. Such a method is referred to as Rao-Blackwellization [17], [18].

In the RB-PF, the estimated states are determined by

$$\hat{\varphi}_k(n) = \sum_{i=1}^{N_s} w_k^i(n)\varphi_k^i(n), \quad \hat{\boldsymbol{x}}_k(n|n) = \sum_{i=1}^{N_s} w_k^i(n)\hat{\boldsymbol{x}}_k^i(n|n)$$

where $w_k^i(n)$ is the weight of the ith particle, $\varphi_k^i(n)$ is the ith particle, and $\hat{\boldsymbol{x}}_k(n|n)$ is the estimated state vector given cumulative measurements $\boldsymbol{z}_k^n = \{\boldsymbol{z}_k(j), \ j = 0, \cdots, n\}$.

A. Particle Filter for Estimating $\varphi_k^i(n)$ and $w_k^i(n)$

We consider a particle filter with N_s *particle streams* defined by

$$\varphi_k^{i,n} \triangleq \{\varphi_k^i(j), \ j = 0, \cdots, n\}, \quad i = 1, \cdots, N_s.$$

The particles $\varphi_k^i(n)$ are generated as random samples from the *importance sampling density* $q(\varphi_k^i(n)|\varphi_k^{i,n-1}, \boldsymbol{z}_k^n)$, which is derived as follow[3]:

$$q(\varphi_k^i(n)|\varphi_k^{i,n-1}, \boldsymbol{z}_k^n)$$
$$= p(\varphi_k^i(n)|\varphi_k^{i,n-1}, \boldsymbol{z}_k^{n-1}) \quad (4)$$
$$= \mathcal{N}\Big(\varphi_k^i(n-1) + T\hat{\dot{\varphi}}_k^i(n|n-1), T^2 \boldsymbol{P}_{\dot{\varphi},k}^i(n|n-1) + T^4/4\sigma_\varphi^2\Big) \quad (5)$$

where (4) is an approximation of $p(\varphi_k^i(n)|\varphi_k^{i,n-1}, \boldsymbol{z}_k^n)$ due to the computability issue,[4] and $\boldsymbol{P}_{\dot{\varphi},k}^i(n|n-1)$ in (5) is the covariance matrix of $\hat{\dot{\varphi}}_k^i(n|n-1)$.

Then the weight is derived as follow:

$$w_k^i(n) \triangleq \frac{p(\varphi_k^{i,n}|\boldsymbol{z}_k^n)}{q(\varphi_k^{i,n}|\boldsymbol{z}_k^n)}$$
$$= \frac{p(\boldsymbol{z}_k^n|\varphi_k^{i,n})p(\varphi_k^{i,n})}{p(\boldsymbol{z}_k^n)} \cdot \frac{1}{q(\varphi_k^{i,n}|\boldsymbol{z}_k^n)}$$
$$= p(\boldsymbol{z}_k(n)|\varphi_k^{i,n}, \boldsymbol{z}_k^{n-1}) \cdot w_k^i(n-1) \quad (6)$$
$$= w_k^i(n-1) \cdot \mathcal{N}\Big(\boldsymbol{z}_k(n); \ \mathbf{H}(\varphi_k^i(n))\hat{\boldsymbol{x}}_k^i(n|n-1),$$
$$\mathbf{H}(\varphi_k^i(n))\boldsymbol{P}_k^i(n|n-1)\mathbf{H}(\varphi_k^i(n))^\mathrm{T} + \boldsymbol{R}_k\Big) \quad (7)$$

where the approximation $q(\varphi_k^{i,n-1}|\boldsymbol{z}_k^n) \approx q(\varphi_k^{i,n-1}|\boldsymbol{z}_k^{n-1})$ is made in (6) again for computability [20].

The particle filter contains a *resampling* procedure when the effective sample size [20] falls below a threshold [18], [21]. We choose the systematic resampling (Algorithm 2 in [20]) for simplicity of implementation.

B. Kalman Filter for Estimating $\hat{\boldsymbol{x}}_k^i(n|n)$

The non-orientation states including position, velocity, acceleration, and angle derivative, can be modeled as linear Gaussian, once the orientation is specified. Hence, the Kalman filter is optimal for estimating $\boldsymbol{x}_k(n)$ given the particle stream $\varphi_k^{i,n}$. Specifically, we use N_s parallel Kalman filters to estimate $\hat{\boldsymbol{x}}_k^i(n), \ i = 1, \cdots, N_s$.

The Kalman filter gain is derived as

$$\boldsymbol{K}_k^i(n) = \boldsymbol{P}_k^i(n|n-1)\mathbf{H}^\mathrm{T}(\varphi_k^i(n))$$
$$\cdot \Big(\mathbf{H}(\varphi_k^i(n))\boldsymbol{P}_k^i(n|n-1)\mathbf{H}^\mathrm{T}(\varphi_k^i(n)) + \boldsymbol{R}_k\Big)^{-1}. \quad (8)$$

The correction steps are given by

$$\hat{\boldsymbol{x}}_k^i(n|n) = \hat{\boldsymbol{x}}_k^i(n|n-1)$$
$$+ \boldsymbol{K}_k^i(n)\Big(\boldsymbol{z}_k(n) - \mathbf{H}(\varphi_k^i(n))\hat{\boldsymbol{x}}_k^i(n|n-1)\Big) \quad (9)$$
$$\boldsymbol{P}_k^i(n|n) = \Big(\mathbf{I} - \boldsymbol{K}_k^i(n)\mathbf{H}(\varphi_k^i(n))\Big)\boldsymbol{P}_k^i(n|n-1). \quad (10)$$

The prediction steps are given by

$$\hat{\boldsymbol{x}}_k^i(n+1|n) = \mathbf{F}\hat{\boldsymbol{x}}_k^i(n|n) \quad (11)$$
$$\boldsymbol{P}_k^i(n+1|n) = \mathbf{F}\boldsymbol{P}_k^i(n|n)\mathbf{F}^\mathrm{T} + \mathbf{G}\boldsymbol{Q}_k\mathbf{G}^\mathrm{T}. \quad (12)$$

The overall RB-PF for IMU-based navigation is described in Algorithm 1.

IV. INTEGRATED IMU/RADIOLOCATION NAVIGATION

In this section, we develop a cooperative navigation algorithm, which fuses the RB-PFs for IMU measurements and the Kalman filter for cooperative radiolocation.

---

[2]The force is normalized by the constant mass of the IMU.

[3]We choose the importance density by assuming the orientation, described by the IMU process model in (2), is a linear Gaussian process [18], [19].

[4]It is difficult to directly compute $p(\varphi_k^i(n)|\varphi_k^{i,n-1}, \boldsymbol{z}_k^n)$, since both $\hat{\dot{\varphi}}_k^i(n|n)$ and $\boldsymbol{P}_{\varphi,k}^i(n|n)$ depend on $\varphi_k^i(n)$, which is not available.

Algorithm 1 Rao-Blackwellization Algorithm for the IMU-based Navigation

Require: $\varphi_k^i(n-1)$, $\hat{\boldsymbol{x}}_k^i(n|n-1)$, $\boldsymbol{P}_k^i(n|n-1)$ and the measurement $\boldsymbol{z}_k(n)$

1: **for** $i = 1, \cdots, N_s$ **do**
2:     Generate particle $\varphi_k^i(n) \sim \mathcal{N}\big(\varphi_k^i(n-1)+T\hat{\dot{\varphi}}_k^i(n|n-1), \; T^2\boldsymbol{P}_{\dot{\varphi},k}^i(n|n-1) + T^4/4\sigma_\varphi^2\big)$
3:     Update the weight $w_k^i(n)$ via (7)
4:     Update $\hat{\boldsymbol{x}}_k^i(n|n)$ and $\boldsymbol{P}_k^i(n|n)$ via (8)–(10)
5:     Predict $\hat{\boldsymbol{x}}_k^i(n+1|n)$ and $\boldsymbol{P}_k^i(n+1|n)$ via (11)–(12)
6: **end for**
7: Normalize the weights by $\widetilde{w}_k^i(n) = w_k^i(n)/\sum_{i=1}^{N_s} w_k^i(n)$, $\forall i = 1, \cdots, N_s$
8: Calculate effective sample size $\widehat{N}_{\text{eff}} = 1/\sum_{i=1}^{N_s}(\widetilde{w}_k^i(n))^2$
9: **if** $\widehat{N}_{\text{eff}} \leq N_T$ **then**
10:     Systematical resampling (cf. [20]) of $\varphi_k^i(n)$, and $w_k^i(n) = 1/N_s$
11: **end if**
12: Calculate the estimated states: $\hat{\varphi}_k(n) = \sum_{i=1}^{N_s} w_k^i(n)\varphi_k^i(n)$ and $\hat{\boldsymbol{x}}_k(n|n) = \sum_{i=1}^{N_s} w_k^i(n)\hat{\boldsymbol{x}}_k^i(n|n)$.
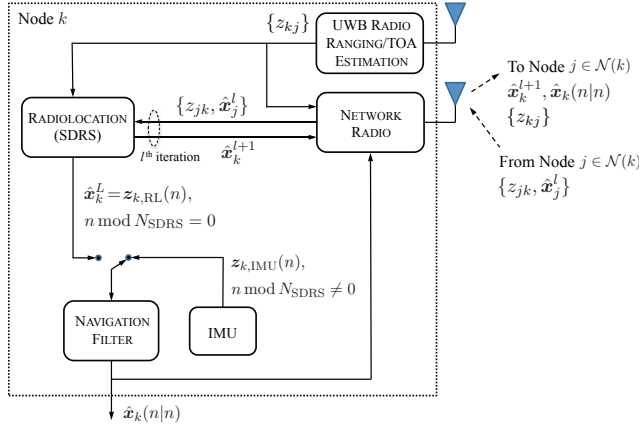

Fig. 1: Cooperative radiolocation and navigation system.

The system digram is shown in Fig. 1. For radiolocation, a steepest descent random start (SDRS) positioning algorithm [14] is adopted to estimate the node's position based on inter-node range measurements. A local navigation filter treats the SDRS estimates and IMU measurements separately to update the final position estimate. We assume that new ranging and SDRS algorithm position estimates are computed after every N_{SDRS} IMU measurements. Specifically, the IMU measurements are treated as nonlinear Gaussian measurements $\boldsymbol{z}_{k,\text{IMU}}(n)$ by the RB-PF when $n \bmod N_{\text{SDRS}} \neq 0$; the SDRS estimates are treated as linear Gaussian measurements $\boldsymbol{z}_{k,\text{RL}}(n)$ by a Kalman filter when $n \bmod N_{\text{SDRS}} = 0$. A detailed description of the radiolocation Kalman filter is given in [14].

Jerk noise standard deviation (STD): σ	5e-5 m/s^3
Angular acceleration noise STD: σ_φ	5e-4 rad/s^2
IMU gyro (angular velocity) noise STD: σ_ω	8.7e-4 rad/s
IMU accelerometer (force) noise STD: σ_f	2e-3 m/s^2
LOS range measurement RMS error: σ_{LOS}	1.5 m
NLOS range measurement RMS error: σ_{NLOS}	9 m
Number of IMU updates per SDRS update: N_{SDRS}	100
Sample time: T	0.1 sec
Total simulation duration	600 sec
Number of simulation runs for error averaging	16
Number of particles: N_s	8

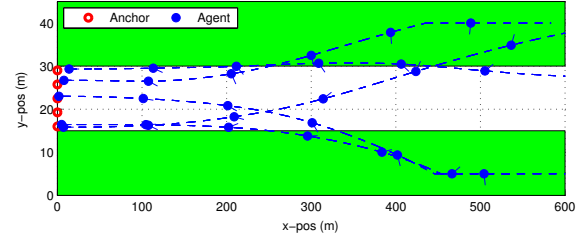TABLE I: Urban corridor simulation parameters

Fig. 2: The urban corridor with mobile nodes trajectories.

V. SIMULATION RESULTS

In this section, we simulate the cooperative IMU-based navigation algorithm in an urban corridor scenario.

The urban corridor is illustrated in Fig. 2, where the street is 15 m wide with buildings 15 m wide on the north and south sides. Five anchor nodes are placed on the west end of the street, and five mobile nodes move at a nominal velocity of 1 m/s heading east, and gradually spread out into the buildings on two sides. The mobile nodes are also rotating themselves, with the small bar on each node denoting the orientation. The movements and rotations are generated according to the Gaussian IMU process model in (1)–(2). Range measurements $z_{k,j}$ are assumed to be LOS when both nodes k, j are in the street, otherwise the measurements are modeled as NLOS. The LOS and NLOS range measurement RMS errors are based on [22] (Fig. 9). The anchor-to-mobile radio range is 100 m. The simulation parameters used are summarized in Table I.

In Fig. 3, we plot all estimation errors averaged over five mobile nodes and 16 simulation runs. We observe that the position error gradually increases as the nodes move towards the east. This is due to the loss of communications when nodes are beyond their radio range to anchors or other mobile nodes, or due to the NLOS conditions when nodes move into buildings.

For comparison, we also plot the average estimation error of an EKF, which uses a single nonlinear filter to estimate all the states. It shows that the RB-PF significantly outperforms the EKF, e.g., it reduces position error more than 10 meters at the end of the corridor. Moreover, the angle estimation using the RB-PF is also much lower, i.e., the error is below 0.2 rad instead of 1.2 rad for the EKF. This is mainly because the
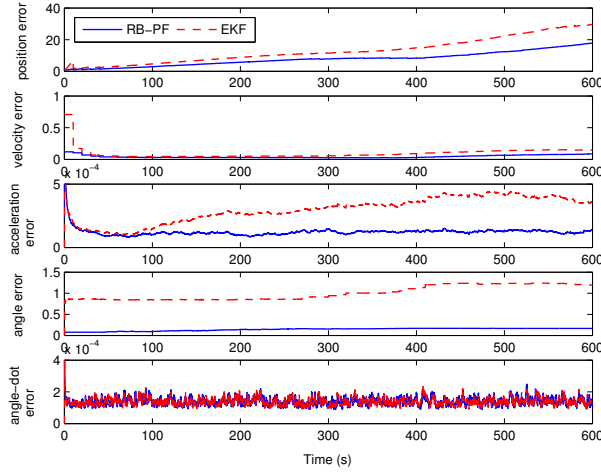
Fig. 3: RB-PF achieves lower averaged estimation errors compared with EKF.

Rao-Blackwellization uses multiple particles to estimate the angle, which results in better convergence compared with a single EKF.

In Fig. 4, we investigate the performance with different extents of node cooperation. Once the mobile nodes move beyond the anchor radio range, the radiolocation relies on inter-mobile range measurements and the IMUs. We consider two settings of mobile-to-mobile radio range: 30 m which results in partial cooperation beyond the middle of the corridor, and 45 m which generally yields full cooperation. We first simulate the urban corridor with buildings (Fig. 2) where both LOS and NLOS conditions exist. In Fig. 4a the 30 m and 45 m range shows that the estimation errors are similar, and the position error with the larger 45 m range is only slightly reduced by 2 m at the end. In Fig. 4b, we removed the two buildings so that LOS signals are always available. The result is a more significant improvement using the 45 m range/full cooperation, i.e., the position error is reduced by 5 m close to the end of the corridor. Hence, the simulation results here support the hypothesis that cooperation among mobile nodes improves the navigation accuracy, especially in the LOS environment.

VI. CONCLUSION

In this paper, we proposed a cooperative IMU-based navigation algorithm using RB-PFs. The IMU measurements and radiolocation information are integrated to improve the navigation accuracy. An urban corridor simulation shows that RB-PFs reduce the position error up to ten meters compared with EKF. Moreover, a significant improvement in angle estimation by a factor of six is observed using the proposed method. The results also demonstrate the importance of node cooperation in navigation, especially in the LOS environment.
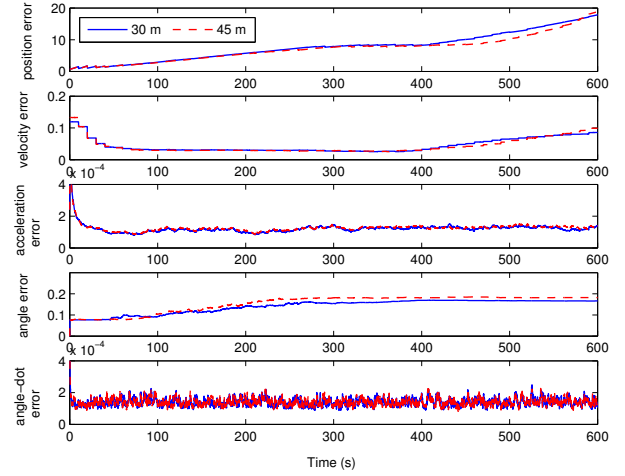
(a) corridor with buildings (mixed LOS and NLOS signals)
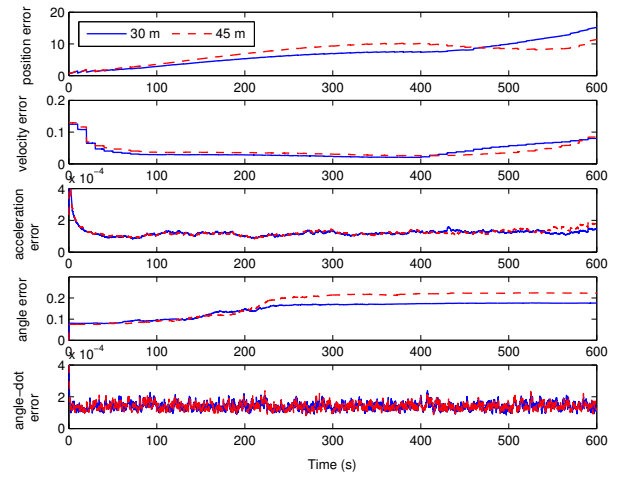
(b) corridor without buildings (only LOS signals)

Fig. 4: Cooperative navigation with larger radio range (more cooperation) outperforms that with smaller radio range (less cooperation) in location accuracy.

VII. RELATION TO PRIOR WORK

This paper has focused on non-GPS navigation, which fuses IMU and radiolocation information. Previous work on IMU-based navigation, e.g., [12], [13], employ a foot-mounted IMU strategy and require step detection to correct the error, which could introduce additional bias and drift. Moreover, most prior research [5], [13]–[16] was limited to Kalman filter or EKF for navigation, which are not as well suited as PFs for the nonlinear IMU model. In this paper, we designed RB-PFs for IMU-based navigation, integrating the radiolocation information, which yields significant improvement on the navigation accuracy.

References

[1] M. Z. Win, A. Conti, S. Mazuelas, Y. Shen, W. M. Gifford, D. Dardari, and M. Chiani, "Network localization and navigation via cooperation," *IEEE Commun. Mag.*, vol. 49, no. 5, pp. 56–62, May 2011.

[2] K. Pahlavan, X. Li, and J.-P. Mäkelä, "Indoor geolocation science and technology," *IEEE Commun. Mag.*, vol. 40, no. 2, pp. 112–118, Feb. 2002.

[3] H. Liu, H. Darabi, P. Banerjee, and J. Liu, "Survey of wireless indoor positioning techniques and systems," *IEEE Trans. Syst., Man, Cybern. C*, vol. 37, no. 6, pp. 1067–1086, Nov. 2007.

[4] Y. Shen, S. Mazuelas, and M. Z. Win, "Network navigation: Theory and interpretation," *IEEE J. Sel. Areas Commun.*, vol. 30, no. 9, pp. 1823–1834, Oct. 2012.

[5] D. H. Titterton and J. L. Weston, *Strapdown Inertial Navigation Technology*. The American Institute of Aeronautics and Astronautics and The Institution of Engineering, 2004.

[6] I. Constandache, R. R. Choudhury, and I. Rhee, "Towards mobile phone localization without war-driving," in *Proc. IEEE Conf. on Computer Commun.*, San Diego, CA, Mar. 2010, pp. 1–9.

[7] C. Ascher, C. Kessler, M. Wankerl, and G. F. Trommer, "Dual IMU indoor navigation with particle filter based map-matching on a smartphone," in *Proc. Int. Conf. on Indoor Positioning and Indoor Navigation*, Zurich, Switzerland, Sep. 2010, pp. 1–5.

[8] J. Han, E. Owusu, L. T. Nguyen, A. Perrig, and J. Zhang, "ACComplice: Location inference using accelerometers on smartphones," in *Proc. Int. Conf. on Commun. Syst. and Netw.*, Bangalore, India, Jan. 2012, pp. 1–9.

[9] S. Gezici, Z. Tian, G. B. Giannakis, H. Kobayashi, A. F. Molisch, H. V. Poor, and Z. Sahinoglu, "Localization via ultra-wideband radios: a look at positioning aspects for future sensor networks," *IEEE Signal Process. Mag.*, vol. 22, no. 4, pp. 70–84, Jul. 2005.

[10] Y. Shen, H. Wymeersch, and M. Z. Win, "Fundamental limits of wideband localization – Part II: Cooperative networks," *IEEE Trans. Inf. Theory*, vol. 56, no. 10, pp. 4981–5000, Oct. 2010.

[11] K. Yu and I. Oppermann, "Performance of UWB position estimation based on time-of-arrival measurements," in *Proc. Int. Workshop on Ultra Wideband Syst.*, Oulu, Finland, May 2004, pp. 400–404.

[12] E. Foxlin, "Pedestrian tracking with shoe-mounted inertial sensors," *IEEE Comput. Graph. Appl.*, vol. 25, no. 6, pp. 38–46, Nov.-Dec. 2005.

[13] A. R. Jiménez, F. Seco, J. C. Prieto, and J. Guevara, "Accurate pedestrian indoor navigation by tightly coupling foot-mounted IMU and RFID measurements," *IEEE Trans. Instrum. Meas.*, vol. 61, no. 1, pp. 178 – 189, Jan. 2012.

[14] R. A. Iltis, "System-level algorithm design for radionavigation using UWB waveforms," in *Proc. Int. Telemetering Conf.*, San Diego, CA, Oct. 2012, pp. 1–10.

[15] I. Skog, "A low-cost GPS aided inertial navigation system for vehicular applications," Master's thesis, Royal Institute of Technology, Stockholm, Sweden, Mar. 2005.

[16] A. R. Jiménez, F. Seco, J. C. Prieto, and J. Guevara, "Indoor pedestrian navigation using an INS/EKF framework for yaw drift reduction and a foot-mounted IMU," in *Workshop on Positioning, Navigation and Commun. (WPNC)*, Dresden, Germany, Mar. 2010, pp. 135 – 143.

[17] F. Gustafsson, F. Gunnarsson, N. Bergman, U. Forsell, J. Jansson, R. Karlsson, and P. J. Nordlund, "Particle filters for positioning, navigation and tracking," *IEEE Trans. Signal Process.*, vol. 50, no. 2, pp. 425–437, Feb. 2002.

[18] B. Ristic, M. S. Arulampalam, and N. Gordon, *Beyond the Kalman Filter: Particle Filters for Tracking Applications*. Norwood, MA: Artech House, 2004.

[19] K. J. Kim, M.-O. Pun, and R. A. Iltis, "Joint carrier frequency offset and channel estimation for uplink MIMO-OFDMA systems using parallel Schmidt Rao-Blackwellized particle filters," *IEEE Trans. Commun.*, vol. 58, no. 9, pp. 2697 – 2708, Sep. 2010.

[20] M. S. Arulampalam, S. Maskell, N. Gordon, and T. Clapp, "A tutorial on particle filters for online nonlinear/non-Gaussian Bayesian tracking," *IEEE Trans. Signal Process.*, vol. 50, no. 2, pp. 174–188, Feb. 2002.

[21] Z. Chen, "Bayesian filtering: From Kalman filters to particle filters, and beyond," McMaster University, Tech. Rep., 2003.

[22] D. Dardari, C.-C. Chong, and M. Z. Win, "Threshold-based time-of-arrival estimators in UWB dense multipath channels," *IEEE Trans. Commun.*, vol. 56, no. 8, pp. 1366–1378, Aug. 2008.